

(February 1998, revised April 1998)

TMUP-HEL-9803

UM-P-98/06

RCHEP-98/02

**Confronting solutions to the atmospheric neutrino anomaly
involving large angle $\nu_\mu \rightarrow \nu_e$ oscillations with
SuperKamiokande and CHOOZ**

R. Foot and R. R. Volkas

*School of Physics**Research Centre for High Energy Physics**The University of Melbourne**Parkville 3052 Australia**(foot@physics.unimelb.edu.au, r.volcas@physics.unimelb.edu.au)*

O. Yasuda

*Department of Physics**Tokyo Metropolitan University**1-1 Minami-Osawa Hachioji, Tokyo 192-0397, Japan**(yasuda@phys.metro-u.ac.jp)*

Abstract

Neutrino oscillation scenarios involving large angle $\nu_\mu \rightarrow \nu_e$ oscillations are disfavoured in the parameter range $\Delta m^2/eV^2 \gtrsim 10^{-3}$ by recent results from the CHOOZ reactor-based $\overline{\nu}_e$ disappearance experiment. For this reason we extend our previous work on up-down asymmetries for various oscillation scenarios by computing up-down asymmetries and the R ratio for the entire conceivable range $10^{-4} - 10^{-1} eV^2$ of Δm^2 . Matter effects in the Earth play a crucial role. We perform a χ^2 fit to the data. We find that, because of the matter effect, the three-flavour maximal mixing model provides a reasonable fit to SuperKamiokande and CHOOZ data provided that the relevant Δm^2 is in the range $4 \times 10^{-4} \lesssim \Delta m^2/eV^2 \lesssim 1.5 \times 10^{-3}$.

Recent data from atmospheric neutrino experiments [1] and especially the SuperKamiokande experiment [1,2] provide very strong evidence for large angle neutrino oscillations. Traditionally the atmospheric neutrino anomaly has been represented by the quantity R , where

$$R \equiv \frac{(N_\mu/N_e)|_{data}}{(N_\mu/N_e)|_{MC}}. \quad (1)$$

The quantities $N_{e,\mu}$ are the numbers of e -like and μ -like events. In addition to an anomalous value for R , the Kamiokande and SuperKamiokande experiments have observed anomalous zenith angle dependence [2,3]. This zenith angle dependence can be represented by the up-down asymmetry parameters [4–8]

$$Y_\alpha^\eta \equiv \frac{(N_\alpha^{-\eta}/N_\alpha^{+\eta})|_{data}}{(N_\alpha^{-\eta}/N_\alpha^{+\eta})|_{MC}} \quad (\alpha = e, \mu). \quad (2)$$

Here $N_\alpha^{-\eta}$ denotes the number of α -like events produced in the detector with zenith angle $\cos \Theta < -\eta$, while $N_\alpha^{+\eta}$ denotes the analogous quantity for $\cos \Theta > \eta$, where η is defined to be positive (note that $\cos \Theta > 0$ for downward going leptons). SuperKamiokande divides the $(-1, +1)$ interval in $\cos \Theta$ into five equal bins. The central bin straddles both the upper and lower hemispheres, and is thus not useful for up-down asymmetry analyses. We therefore choose $\eta = 0.2$ in order to utilise all the data in the other four bins.

When comparing the measured results for R and the Y 's with predictions from a specific neutrino oscillation model, the numerators are replaced by calculated predictions from the models, while the denominators remain as the no-oscillation predictions. Note that systematic uncertainties for up-down asymmetries are expected to be smaller than for R , because the latter depends on the relative flux of ν_μ to ν_e .

The utility of using up-down asymmetries as a diagnostic tool was emphasised in Ref. [5], where up-down asymmetries were computed for various neutrino oscillation solutions to the atmospheric neutrino anomaly. The analysis of Ref. [5] focussed on the energy dependence of up-down asymmetries. By contrast, in Refs. [6,7] we followed (super)Kamiokande and considered particular cuts in energy.

In Ref. [7], we analysed four representative cases:

- (A) Maximal $\nu_\mu - \nu_\tau$ mixing [9].
- (B) Maximal $\nu_\mu - \nu_e$ mixing [10].
- (C) Threefold maximal mixing [11,12] amongst ν_e , ν_μ and ν_τ .
- (D) Massless neutrinos with violation of the Equivalence Principle or breakdown of Lorentz invariance [13]. The case of maximal $\nu_e - \nu_\mu$ oscillations [14] was considered for definiteness.

In Ref. [7], we focussed on the region of parameter space $\Delta m^2/eV^2 > 2 \times 10^{-3}$. However, large angle $\nu_\mu \rightarrow \nu_e$ oscillations are now disfavoured in this parameter range because of recent results from the CHOOZ reactor-based $\bar{\nu}_e$ disappearance experiment [15]. This experiment disfavours maximal $\nu_e - \nu_\mu$ mixing for $\Delta m^2/eV^2 > 0.9 \times 10^{-3}$ at 90% C.L. Thus it is important to discuss the parameter space region $\Delta m^2/eV^2 < 2 \times 10^{-3}$. In Ref [7] we neglected matter effects [16] due to neutrino oscillations through the Earth. However, it

turns out that this is *not* a valid approximation for the 2-flavour cases for multi-GeV (sub-GeV) neutrinos unless $\Delta m^2/eV^2 \gtrsim 10^{-2}$ (10^{-3}), and is never a good approximation for model C. Thus the purpose of this paper is to reexamine the up-down asymmetries and R for the entire conceivable range of interest for Δm^2 (i.e. $\Delta m^2/eV^2 > 10^{-4}$). We will numerically integrate the Schrödinger equation for neutrino evolution including the matter effects, taking the density profile of the Earth from Ref. [17]. We will show that for the two flavour $\nu_\mu \rightarrow \nu_e$ oscillation models B and D the matter effects suppress the oscillations and do not improve the fit of these models to the data. *Interestingly, however, for the 3-flavour model C the matter effects actually improve the fit of the model to the data.* Although this model does not fit the data as well as model A, we will show that this model does provide an acceptable fit to the SuperKamiokande and CHOOZ data for a range of Δm^2 .

Our methodology is similar to our previous paper [7] except that we have used the inclusive cross section given in Ref. [18] for the multi-GeV analysis. Although this cross section is not completely satisfactory for calculating absolute event rates because it does not incorporate low Q^2 effects such as the Δ resonance production, it is a good enough approximation for calculating ratios of event rates such as up-down asymmetries and R . We also include results for case A, even though it does not involve ν_e , because it will be interesting to compare cases A and C. [For a comparative analysis of case A and the somewhat similar large angle $\nu_\mu \rightarrow \nu_s$ solution (where ν_s is a sterile neutrino), see Ref, [19]]. We are now able to improve on the analysis of Ref. [7] in another respect, because we have been fortunate to obtain the detection efficiency functions from the SuperKamiokande collaboration.

Our results are given in Figures 1-6 [20,21], together with preliminary results from superKamiokande (corresponding to 414 days of live running) [2]

$$\begin{aligned} R(\text{sub-GeV}) &= 0.61 \pm 0.03 \pm 0.05, \quad R(\text{multi-GeV}) = 0.67 \pm 0.06 \pm 0.08, \\ Y_\mu^{0.2}(\text{sub-GeV}) &= 0.78 \pm 0.06, \quad Y_\mu^{0.2}(\text{multi-GeV}) = 0.49 \pm 0.06, \\ Y_e^{0.2}(\text{sub-GeV}) &= 1.13 \pm 0.08, \quad Y_e^{0.2}(\text{multi-GeV}) = 0.83 \pm 0.13. \end{aligned} \quad (3)$$

Note that only statistical errors are given for the up-down asymmetries since they should be much larger than possible systematic errors at the moment.

Figures 1,2 show that all of the models A,B,C,D can provide an acceptable fit to R . However the up-down asymmetries $Y_{e,\mu}$ clearly distinguish the models. The only cases which can provide an acceptable fit to all of the data are A and C. Indeed, the $Y_{e,\mu}$ and R values for model C are quite similar to model A for low Δm^2 . To understand this point, consider the Schrödinger equation for neutrino evolution in model C including matter effects,

$$i \frac{d}{dx} \begin{bmatrix} \nu_e(x) \\ \nu_\mu(x) \\ \nu_\tau(x) \end{bmatrix} = \frac{\Delta m^2}{2E} \begin{bmatrix} A(x) + 1/3 & 1/3 & 1/3 \\ 1/3 & 1/3 & 1/3 \\ 1/3 & 1/3 & 1/3 \end{bmatrix} \begin{bmatrix} \nu_e(x) \\ \nu_\mu(x) \\ \nu_\tau(x) \end{bmatrix}, \quad (4)$$

where x is the distance travelled, E the neutrino energy, Δm^2 the larger of the two squared-mass differences in model C and $\nu_{e,\mu,\tau}(x)$ the wave-functions of the neutrinos. The quantity $A(x)$ is related to the effective potential difference generated through the matter effect:

$$A(x) = \frac{2E}{\Delta m^2} \sqrt{2} G_F N_e(x) \simeq 2.9 \times 10^{-4} \cdot \left[\frac{E/\text{GeV}}{\Delta m^2/\text{eV}^2} \right] \left[\frac{\rho(x)}{4 \text{ g/cm}^3} \right], \quad (5)$$

where G_F is the Fermi constant, $N_e(x)$ the number density of electrons along the path of the neutrino and $\rho(x)$ the mass density of the earth (in deriving the right hand side of Eq.(5) we have assumed that the average number of protons per nucleon is approximately constant ~ 0.48). For antineutrinos the sign of $A(x)$ is reversed.

For $E/\Delta m^2$ values leading to large matter effects ($A \gg 1/3$), ν_e oscillations are suppressed. The system in this case exhibits approximate two flavour $\nu_\mu \rightarrow \nu_\tau$ maximal oscillations with

$$P(\nu_\mu \rightarrow \nu_\tau) = 1 - \sin^2 \left[\frac{2}{3} \times 1.27 \frac{(L/km)(\Delta m^2/eV^2)}{(E/GeV)} \right]. \quad (6)$$

This qualitatively explains why R, Y for case C are similar to case A for $\Delta m^2/eV^2 \gtrsim 3 \times 10^{-3}$. From Eq.(6), observe that for a given Δm^2 the oscillation length of $\nu_\mu \rightarrow \nu_\tau$ is not the same as the oscillation length for genuine two flavour oscillations - it is 1.5 times longer. This explains why the multi-GeV R and Y_μ for model C are displaced relative to model A. Finally note that in the large $\Delta m^2/E$ limit, the Y_μ asymmetry does not approach 1 in model C. In fact, one can show by explicit computation that in the large $\Delta m^2/E$ limit, the muon neutrino survival probability is related to the vacuum survival probability by

$$P(\nu_\mu \rightarrow \nu_\mu)(A) = P(\nu_\mu \rightarrow \nu_\mu)(A = 0) - \frac{1}{6} \left(1 - \cos \frac{2 \Delta m^2 A L}{3 \cdot 2E} \right). \quad (7)$$

Note that $\Delta m^2 A/E$ is independent of Δm^2 and E and thus it turns out that there is no range of parameters where matter effects can be neglected for atmospheric neutrinos in model C.

We now perform a χ^2 analysis to determine the preferred region of Δm^2 for model C. We will not consider models B and D because they obviously lead to bad fits. We first define a χ^2 function for atmospheric data: [22]

$$\chi_{atm}^2 = \sum_E \left[\left(\frac{R^{SK} - R^{th}}{\delta R^{SK}} \right)^2 + \left(\frac{Y_\mu^{SK} - Y_\mu^{th}}{\delta Y_\mu^{SK}} \right)^2 + \left(\frac{Y_e^{SK} - Y_e^{th}}{\delta Y_e^{SK}} \right)^2 \right], \quad (8)$$

where the sum is over the sub-GeV and multi-GeV cases, the measured SuperKamiokande values and errors are denoted by the superscript “SK” and the theoretical predictions for the quantities are labelled by “th”. The $\eta = 0.2$ choice is understood for the up-down asymmetries. There are 6 pieces of data in χ^2 and 1 adjustable parameter, Δm^2 , leaving 5 degrees of freedom. [Note that in the present paper we consider $|U_{\alpha j}|^2 = 1/3$ ($\alpha = e, \mu, \tau$, $j = 1, 2, 3$) for model C and thus the mixing angles do not constitute free parameters].

The solid line in Fig. 7 displays χ_{atm}^2 as a function of Δm^2 for model C (also shown is χ_{atm}^2 for the Y asymmetries only). The CHOOZ experiment disfavours $\Delta m^2/eV^2 \gtrsim 10^{-3}$ for large angle $\nu_\mu \rightarrow \nu_e$ oscillations [15]. In order to incorporate the CHOOZ results, we define another χ^2 :

$$\chi_{CHOOZ}^2 = \sum_i \left(\frac{x_i - y_i}{\delta x_i} \right)^2. \quad (9)$$

The sum is over 12 energy bins of data (in the above equation x_i are experimental values from Figure 5b of Ref. [15] and y_i are the corresponding theoretical predictions) [23]. The

short-dashed line in Fig.7 displays χ^2_{CHOOZ} as a function of Δm^2 for model C. Figure 8 plots $\chi^2_{atm} + \chi^2_{CHOOZ}$. The 3σ allowed range for the atmospheric data plus CHOOZ is

$$4 \times 10^{-4} \lesssim \Delta m^2/eV^2 \lesssim 1.5 \times 10^{-3}. \quad (10)$$

The best fit point at $\Delta m^2 \simeq 8 \times 10^{-4} eV^2$ gives $\chi^2_{min} \simeq 23$ for 17 degrees of freedom which implies an allowed C.L. of 16% for model C to explain the atmospheric data while simultaneously being consistent with CHOOZ.

We have also performed a χ^2 fit for model C to the solar neutrino data for the parameter space of Ref. [12]. This model predicts an energy independent solar electron neutrino flux reduction of 5/9 (this leads to predictions for the solar neutrino experiments which are reduced by a factor 5/9, except for (super)Kamiokande where neutral current effects must be incorporated). We have used the most recent results for Homestake ($2.55 \pm 0.14 \pm 0.14 SNU$) [24], GALLEX($76.4 \pm 6.3^{+4.5}_{-4.9} SNU$) [25], SAGE ($69.9^{+8.9}_{-8.7} SNU$) [26]. For Kamiokande (SuperKamiokande) we have used the 8(16) energy bins given in Ref. [27] (Ref. [28]). We choose to leave the boron flux as a free parameter [10,12] and neglect the small theoretical errors of the other fluxes. We consider two solar models for definiteness, BP95 [29] and TCL [30]. We find that $\chi^2_{solar}(min) = 44$ for BP95 solar model and $\chi^2_{solar}(min) = 33$ for TCL solar model. With the boron flux as a free-parameter, there are $27 - 1 = 26$ degrees of freedom. Thus, the overall fit of model C to the solar+atmospheric+CHOOZ experiments turns out to be reasonable with $\chi^2_{min} = 67$ (BP95) and 56 (TCL) for 43 degrees of freedom which corresponds to an allowed C.L. of 1% (BP95) and 10% (TCL).

In conclusion, we have extended the analysis of Ref. [7] to include low values of $\Delta m^2/eV^2$. This is important for models which have large angle $\nu_\mu \rightarrow \nu_e$ oscillations because of the recent CHOOZ results. Out of the three cases (B, C and D) which involve ν_e , only the three-flavour maximal mixing model (case C) provides a reasonable fit to the up-down asymmetries and R ratios while being consistent with CHOOZ. We thus reach the important conclusion that the most favoured solutions to the atmospheric neutrino anomaly in the light of CHOOZ are: (i) large angle or maximal $\nu_\mu \rightarrow \nu_\tau$ oscillations (case A), (ii) large angle or maximal $\nu_\mu \rightarrow \nu_s$ oscillations [19] and, (iii) three-flavour maximal mixing (case C) with $\Delta m^2 \sim 8 \times 10^{-4} eV^2$ (sufficiently small departures from three-flavour maximal mixing would also of course be allowed). If (i) is true then the planned Japanese long baseline neutrino oscillation experiment may or may not see a signal (see Ref. [19]), if (ii) is true then present data suggest that they should see a signal [19], and if three-flavour maximal mixing is correct then the Japanese long baseline experiment has no chance to see a signal. Finally note that if model C is correct then the Kamland experiment should see a positive signal.

ACKNOWLEDGMENTS

O.Y. was supported in part by a Grant-in-Aid for Scientific Research of the Ministry of Education, Science and Culture, #09045036. O.Y. would like to thank T. Kajita for useful communications and the participants of the Neutrino Symposium at Hachimantai, Japan, on Nov.28-30 1997 for discussions. R.F. and R.R.V. are supported by the Australian Research Council. R.F. would like to thank P. Harrison for useful correspondence.

REFERENCES

- [1] Y. Totsuka, Talk at *XVIII International Symposium on Lepton-Photon Interactions*, July, Hamburg, Germany (<http://www.desy.de/lp97-docs/proceedings/lp22/lp22.ps>).
- [2] E. Kearns, Talk at *News about SNUS*, ITP Workshop, Santa Barbara, Dec. 1997, <http://www.itp.ucsb.edu/online/snu/kearns/oh/all.html>).
- [3] Kamiokande Collaboration, Y. Fukuda et al., *Phys. Lett.* **B335**, 237 (1994).
- [4] J. Bunn, R. Foot and R. R. Volkas, *Phys. Lett.* **B413**, 109 (1997).
- [5] J. W. Flanagan, J. G. Learned and S. Pakvasa, *Phys. Rev.* **D57**, 2649 (1998).
- [6] R. Foot, R. R. Volkas and O. Yasuda, *Phys. Rev.* **D57**, 1345 (1998).
- [7] R. Foot, R. R. Volkas and O. Yasuda, [hep-ph/9710403](http://arxiv.org/abs/hep-ph/9710403), *Phys. Lett.* **B** (in press).
- [8] G. L. Fogli et al., [hep-ph/9711421](http://arxiv.org/abs/hep-ph/9711421).
- [9] J. G. Learned, S. Pakvasa and T. J. Weiler, *Phys. Lett.* **B207**, 79 (1988); V. Barger and K. Whisnant, *Phys. Lett.* **B209**, 365 (1988); K. Hidaka, M. Honda and S. Midorikawa, *Phys. Rev. Lett.* **61**, 1537 (1988).
- [10] A. Acker and S. Pakvasa, *Phys. Lett.* **B397**, 209 (1997); A. Acker, J. G. Learned, S. Pakvasa and T. Weiler, *Phys. Lett.* **B298**, 149 (1993).
- [11] C. Giunti, C. W. Kim and J. D. Kim, *Phys. Lett.* **B352**, 357 (1995). See also R. N. Mohapatra and S. Nussinov, *Phys. Lett.* **B346**, 75 (1995).
- [12] P. F. Harrison, D. H. Perkins and W. G. Scott, *Phys. Lett.* **B396**, 186 (1997); *Phys. Lett.* **B349**, 137 (1995).
- [13] M. Gasperini, *Phys. Rev.* **D38**, 2635 (1988); A. Halprin and C. N. Leung, *Phys. Rev. Lett.* **67**, 1833 (1991); K. Iida, H. Minakata and O. Yasuda, *Mod. Phys. Lett.* **A8**, 1037 (1993); S. Coleman and S. L. Glashow, *Phys. Lett.* **B405**, 249 (1997); S. L. Glashow et al., *Phys. Rev.* **D56**, 2433 (1997); J. Pantaleone, A. Halprin and C. N. Leung, *Phys. Rev.* **D47**, 4199 (1993); J. R. Mureika and R. B. Mann, *Phys. Rev.* **D54**, 2761 (1996).
- [14] In this case the survival probability is given by $P_{ee} = P_{\mu\mu} = 1 - \sin^2 \frac{\delta v}{2} EL$ and the transition probability is $P_{e\mu} = P_{\mu e} = \sin^2 \frac{\delta v}{2} EL$ (where E and L are the energy of the neutrino and the distance travelled respectively).
- [15] CHOOZ Collaboration, M. Apollonio et al., [hep-ex/9711002](http://arxiv.org/abs/hep-ex/9711002).
- [16] L. Wolfenstein, *Phys. Rev.* **D17**, 2369 (1978); S. P. Mikheyev and A. Yu Smirnov, *Yad. Fiz.* **42**, 1441 (1985) [*Sov. J. Nucl. Phys.* **42**, 913 (1985)]; *Nuovo Cim.* **C9**, 17 (1986).
- [17] F. Stacey, *Physics of the Earth*, 2nd ed. (J. Wiley and Sons, Chichester, 1977).
- [18] V. Barger and R. J. N. Phillips, *Collider Physics* (Addison-Wesley, 1987), p.153.
- [19] R. Foot, R.R. Volkas and O. Yasuda, [hep-ph/9801431](http://arxiv.org/abs/hep-ph/9801431) (to appear in *Phys. Rev. D*).
- [20] Note that we have included the effects of an estimated 7% [2] misidentification of muons as electrons in the multi-GeV analysis. For this reason $\nu_\mu \rightarrow \nu_\tau$ oscillations can slightly affect the Y_e asymmetries.
- [21] In our numerical work we found some small oscillations (less than a few percent) which we have smoothed out in the figures.
- [22] The statistical procedure we employ is approximate in the sense that ratios of Gaussian-distributed quantities are only approximately Gaussian themselves [see e.g. G. L. Fogli and E. Lisi, *Phys. Rev.* **D52**, 2775 (1995)]. The validity of using ratios increases as the fractional errors decrease. Since SuperKamiokande is a high statistics experiment, our procedure is accurate within a sufficiently small region around the best fit point

provided this point gives a reasonably good fit (we estimate that it is approximately valid within the 3σ region around the best fit).

- [23] Some consequences of the CHOOZ experiment have been discussed in: H. Minakata and O. Yasuda, hep-ph/9712291; M. Narayan, G. Rajasekaran and S. U. Sankar, hep-ph/9712409.
- [24] K. Lande (Homestake Collab.), Proceedings of 17th International Conference on Neutrino Physics and Astrophysics, Ed. K. Enqvist et. al. (World Scientific, 1996).
- [25] W. Hampel (Gallex Collab.), Talk at *News about SNUS*, ITP Workshop, Santa Barbara, Dec. 1997, <http://www.itp.ucsb.edu/online/snu/hampel/oh/all.html>.
- [26] V. Gavrin (SAGE Collab.), Talk at *News about SNUS*, ITP Workshop, Santa Barbara, Dec. 1997, <http://www.itp.ucsb.edu/online/snu/gavrin/oh/all.html>.
- [27] Kamiokande Collaboration, Y. Fukuda et. al., Phys. Rev. Lett. **77**, 1683 (1996).
- [28] R. Svoboda (SuperKam collab.), Talk at *News about SNUS*, ITP Workshop, Santa Barbara, Dec. 1997, <http://www.itp.ucsb.edu/online/svoboda/oh/all.html>.
- [29] J. N. Bahcall and M. H. Pinsonneault, Rev. Mod. Phys. 67, 781 (1995).
- [30] S. Turck-Chieze and I. Lopes, Astrophys. J. 408, 347 (1993).

Figure Captions

Figure 1. The sub-GeV R as a function of $\Delta m^2/eV^2$ [$(\delta v/2)kmGeV$] for models A (solid line), B (dashed-dotted line), C (dashed line) [D (dotted line)]. The usual SuperKamiokande sub-GeV momentum cuts have been employed. The horizontal long-dashed lines are the preliminary SuperKamiokande data $\pm 1\sigma$ statistical errors.

Figure 2. Same as Figure 1 except for SuperKamiokande multi-GeV case.

Figure 3. The sub-GeV up-down e -type asymmetry $Y_e^{0.2}$ as a function of $\Delta m^2/eV^2$ [$(\delta v/2)kmGeV$] for models A (solid line), B (dashed-dotted line), C (dashed line) [D (dotted line)]. The usual SuperKamiokande sub-GeV momentum cuts have been employed. The horizontal long-dashed lines are the preliminary SuperKamiokande data $\pm 1\sigma$ statistical errors.

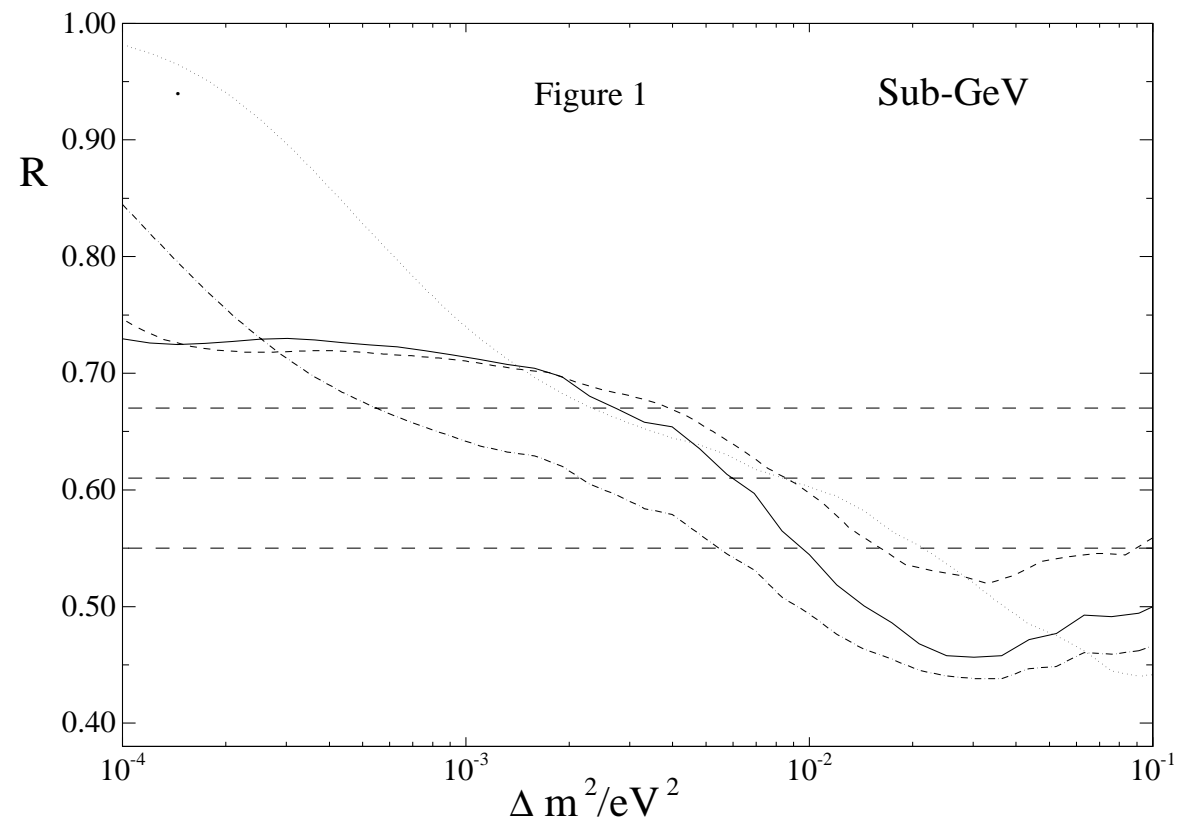
Figure 4. Same as Figure 3 except for muons instead of electrons.

Figure 5. Same as Figure 3 except for multi-GeV sample.

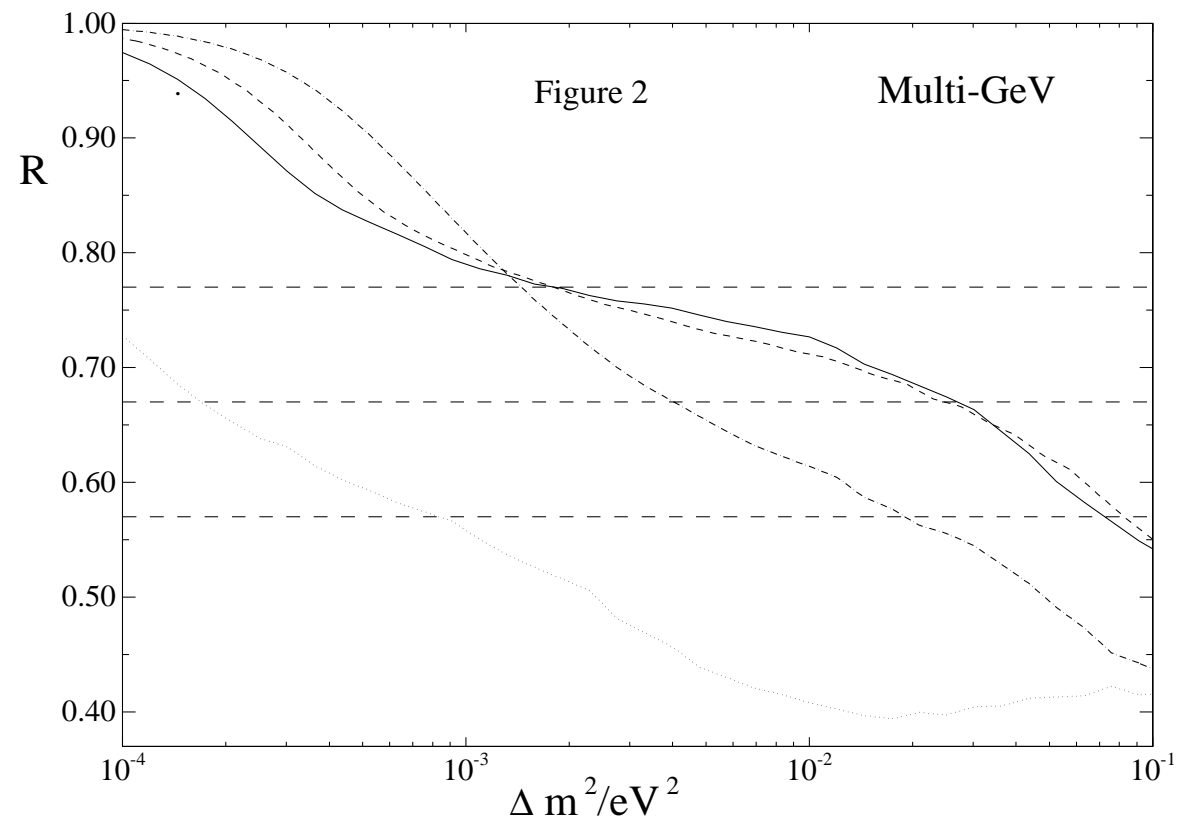
Figure 6. Same as Figure 3 except for muons and for multi-GeV sample.

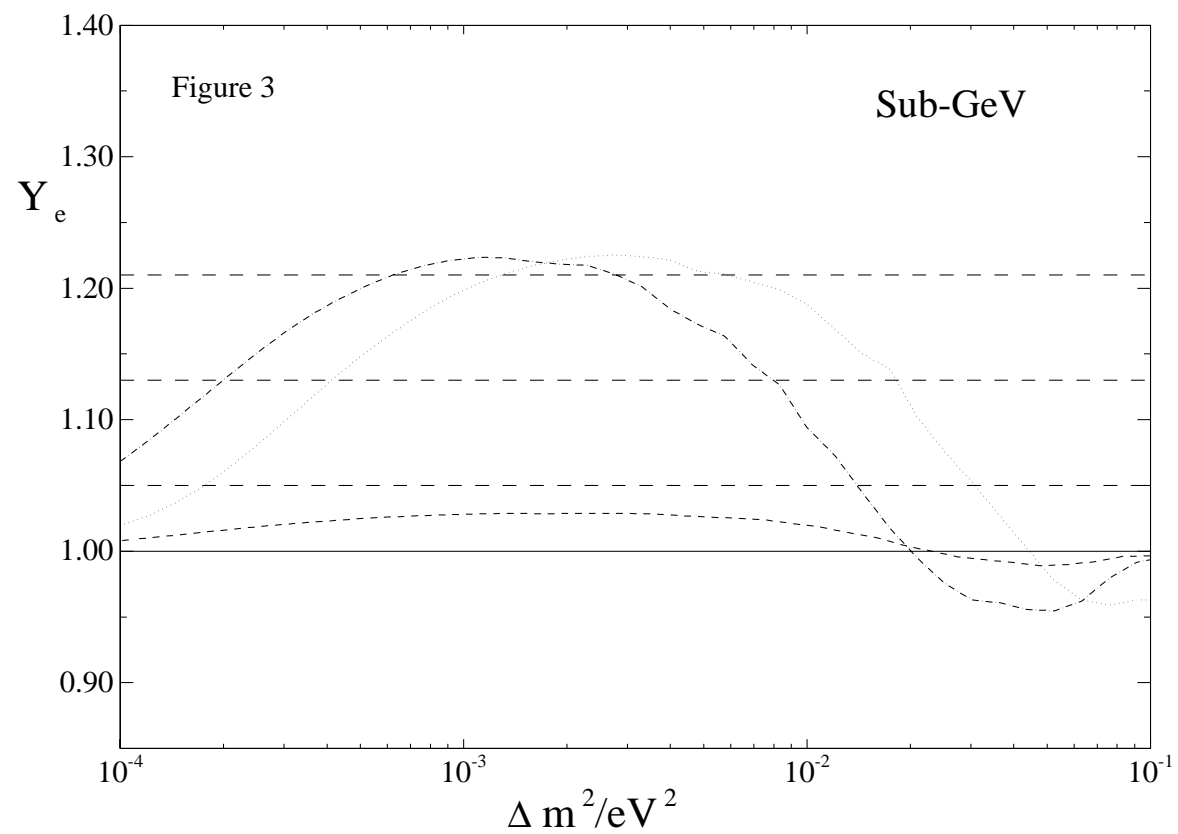
Figure 7. χ^2 fit as a function of Δm^2 to the SuperKamiokande atmospheric data for Model C. The solid line includes both R and up-down asymmetries whereas the dashed line includes only the up-down asymmetries. The χ^2 for the CHOOZ reactor data (dotted line) is also shown.

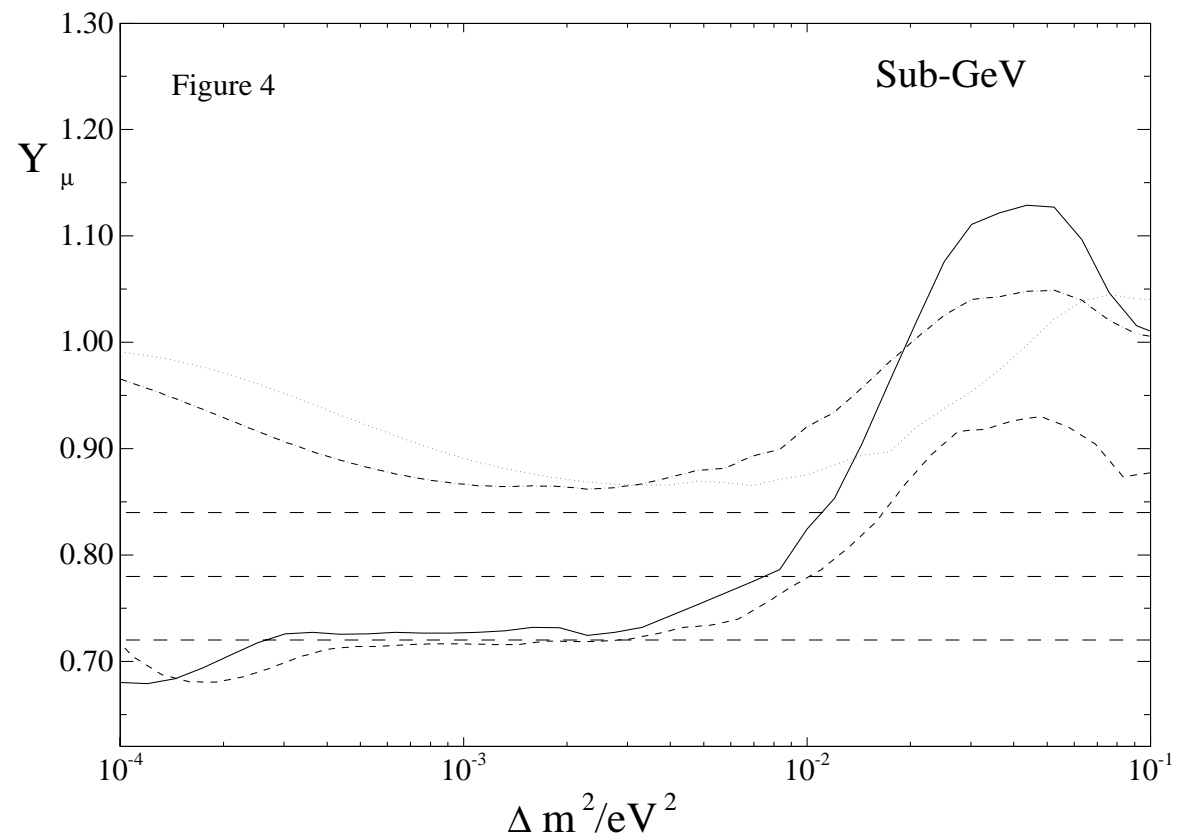
Figure 8. Combined χ^2 fit as a function of Δm^2 to the SuperKamiokande atmospheric data and the CHOOZ reactor data for model C.

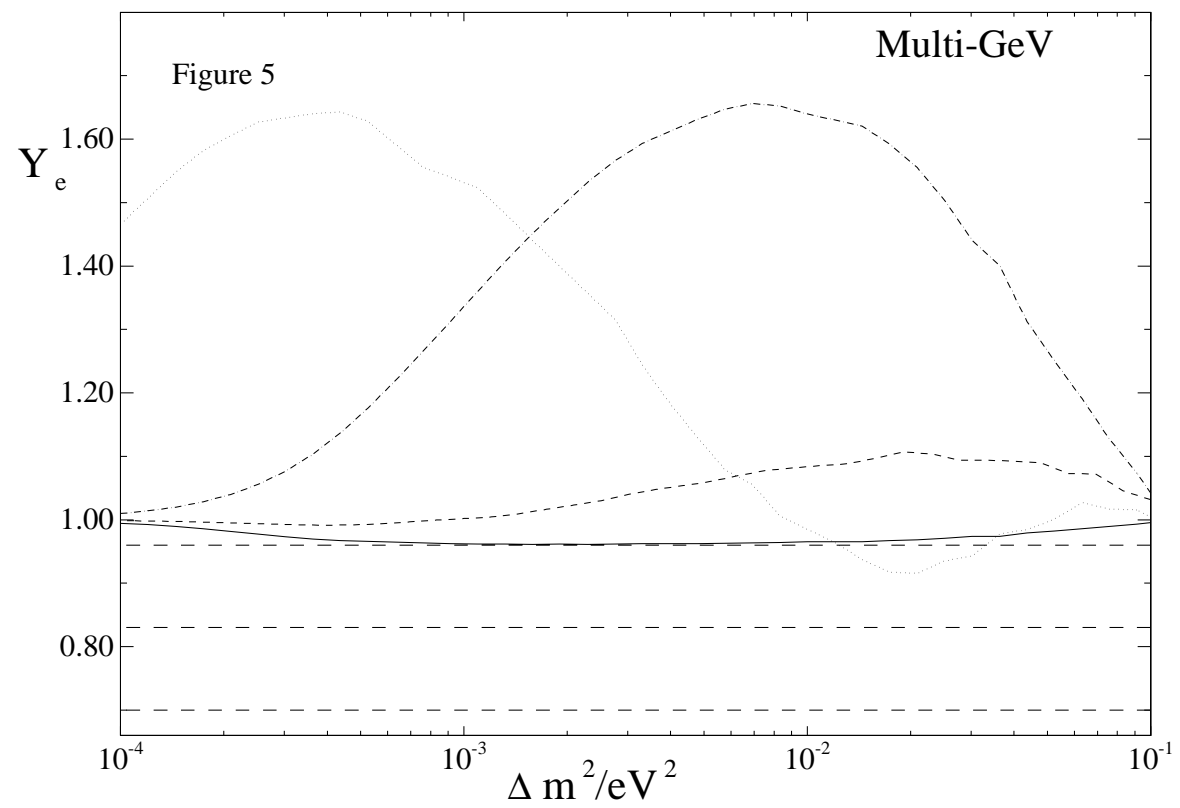


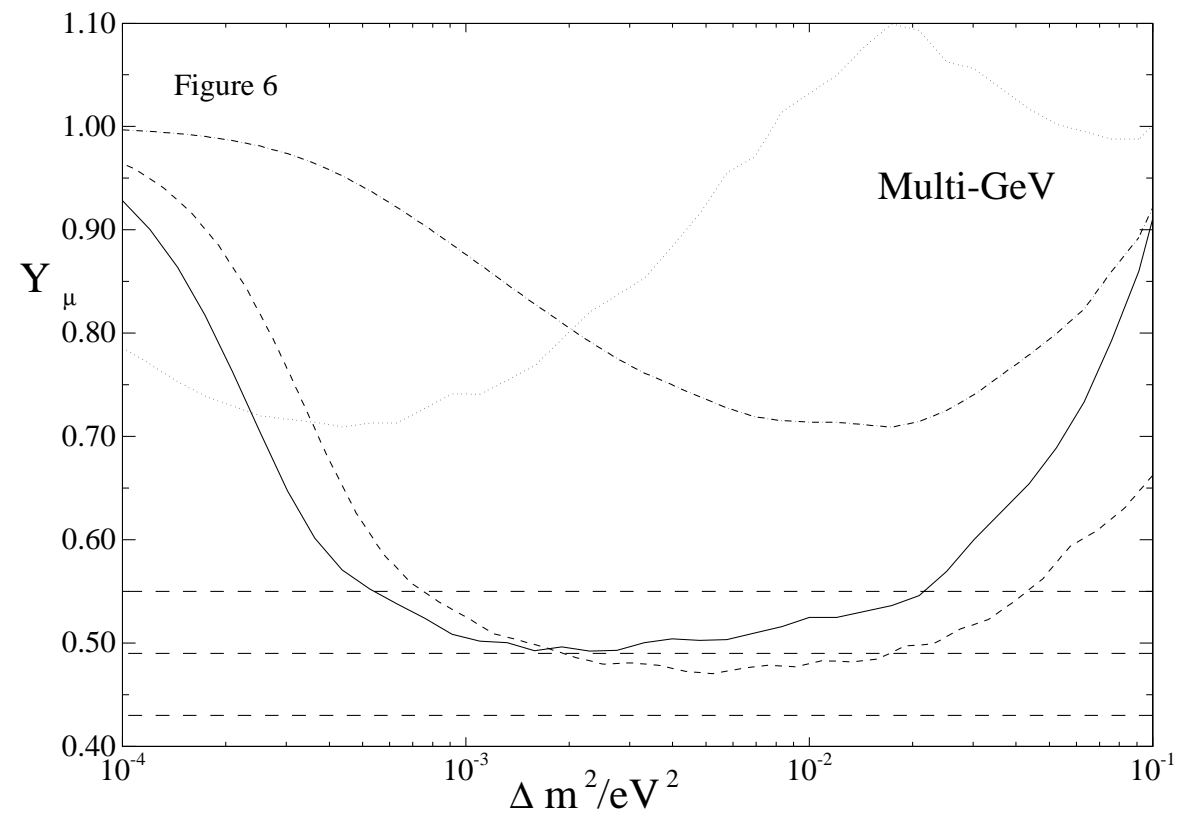
10











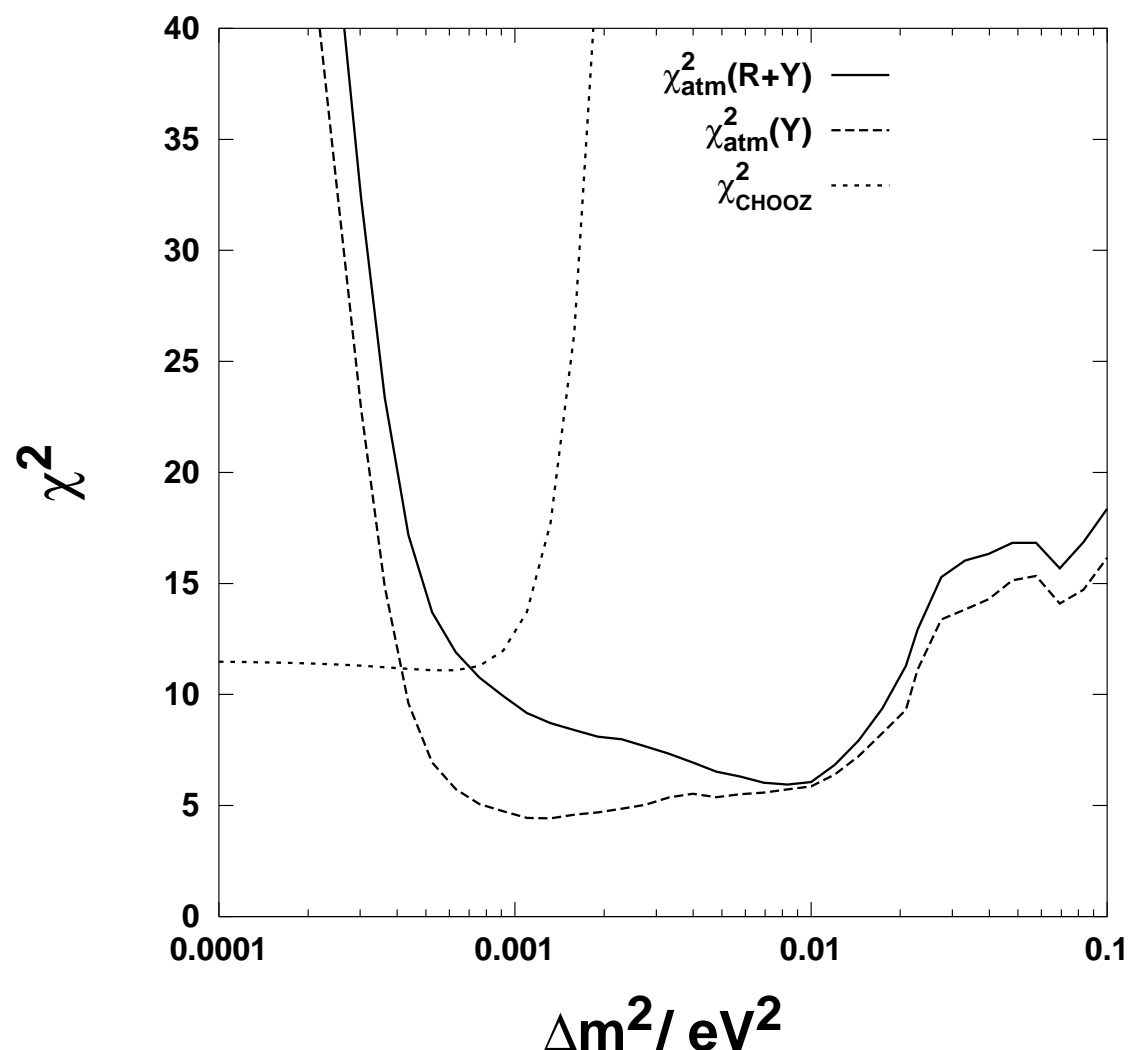


Fig.7

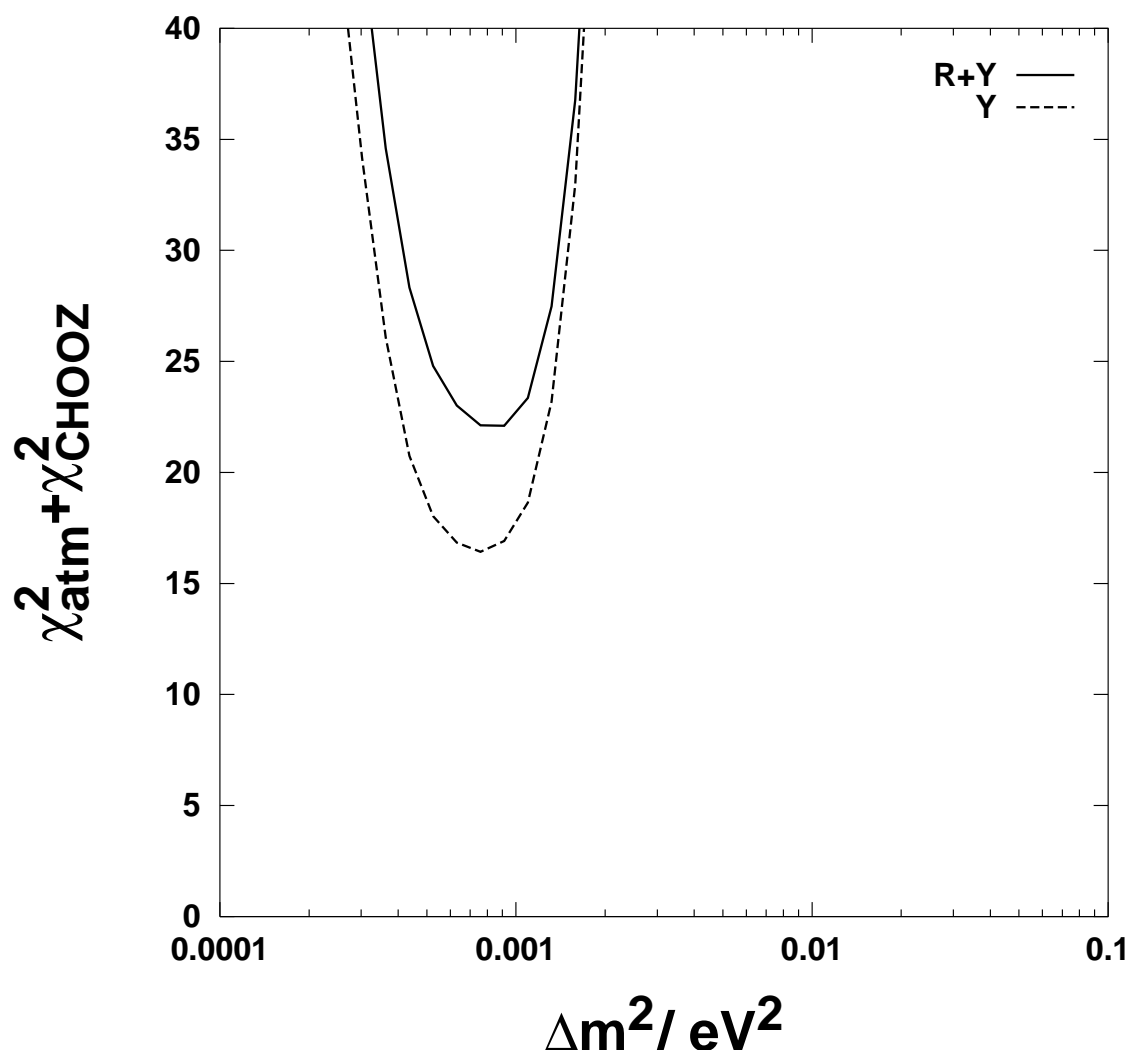


Fig.8